



*Supplement of*

## **Volcanic stratospheric sulfur injections and aerosol optical depth during the Holocene (past 11 500 years) from a bipolar ice-core array**

**Michael Sigl et al.**

*Correspondence to:* Michael Sigl ([michael.sigl@climate.unibe.ch](mailto:michael.sigl@climate.unibe.ch))

The copyright of individual parts of the supplement might differ from the article licence.

**Table S1: List of abbreviations:**

AICC2012: Antarctic Ice Core Chronology 2012 (Veres et al. 2013)

ANT12k: Antarctica Volcanic Sulfate Stack (N=3 ice cores) covering the past 11,500 years

AVS2k: Antarctica Volcanic Sulfate Stack (N≤14 ice cores) covering the past 2,000 years (Sigl et al., 2014)

BCE: Before the Common Era

BP: Before present (defined as before 1950 CE)

CE: Common Era; notation for the Gregorian calendar, equivalent to Anno Domini (AD)

DEP: Dielectric Profiling; non-destructive method using rapid scanning of ice cores' electric permittivity and conductivity with the latter related mainly to acidity, salt and ammonia concentrations of ice cores

DRI: Desert Research Institute

ECHAM5-HAM: Coupled aerosol-climate model in which model processes related to sulfate aerosols are calculated by the aerosol microphysical module HAM adopted for volcanic simulations

EDC: EPICA Dome C deep ice core from East Antarctica

EDML: EPICA Dronning Maud Land deep ice core from East Antarctica

EPICA: European Project for Ice Coring in Antarctica; a multinational European project for deep ice core drilling in Antarctica.

EVA: Easy Volcanic Aerosol (EVA) forcing generator (Toohey et al., 2016b)

eVolv2k: Ice-core volcanic eruption catalogue (500 BCE – 1900 CE) reconstructed from synchronized bipolar ice-core records

FIC: Fast ion chromatography; high-resolution ion chromatography method using a melter-based continuous flow analysis system for the analysis of sulfate and other ionic species

: Greenhouse gases (e.g., H<sub>2</sub>O, CO<sub>2</sub>, CH<sub>4</sub>, N<sub>2</sub>O, O<sub>3</sub>)

GICC05: Greenland Ice Core Chronology 2005; annual-layer counted chronology developed from the three Greenland ice cores NGRIP, GRIP, and DYE-3

GISP2: Greenland Ice Sheet Project Two deep ice core from Central Greenland

GRIP: Greenland Ice Core Project deep ice core from Central Greenland

GVP: Global Volcanism Program; a catalog of Holocene and Pleistocene volcanoes, and eruptions from the past 12,000 years. Smithsonian Institution, [https://volcano.si.edu/gvp\\_about.cfm](https://volcano.si.edu/gvp_about.cfm)

HolVol v.1.0: Ice-core volcanic eruption catalogue (9500 – 1900 CE; Holocene) reconstructed from synchronized bipolar ice-core records

IC: Ion chromatography

ICPMS: Inductively coupled plasma mass spectrometry

IPCC: Intergovernmental Panel on Climate Change

LGM: Last Glacial Maximum

MAD: Median of absolute deviation

NEEM-2011-S1: Intermediate length ice-core drilled at the North Greenland Eemian Ice Drilling (NEEM) deep ice-core drilling site covering the time period 87-2011 CE.

NGRIP: North Greenland Ice Core Project deep ice core from North Greenland (also NorthGRIP)

NH: Northern hemisphere

NHET: Northern Hemisphere Extratropics (23.5-90°N)

NS1-2011: Annual-layer counted chronology developed from the NEEM-2011-S1 ice core

PMIP: Paleoclimate Model Intercomparison Project

RF: Radiative forcing (in W m<sup>-2</sup>)

RM: Running median

RRM: Reduced running median (after removal of all volcanic peaks)

SAOD: Stratospheric aerosol optical depth (at 550 nm wavelength)

SH: Southern hemisphere

SHEET: Southern Hemisphere Extratropics (23.5-90°S)

TE-CFA: Trace Element – Continuous Flow Analysis; high-resolution mass spectrometry method using a melter-based continuous flow analysis system for the analysis of multiple trace elements (e.g. sulfur) and other impurities

TUNU2013: Intermediate length ice-core drilled in NE-Greenland covering the time period 270-2013 CE.

VEI: Volcanic Explosivity Index

VSSI: Volcanic stratospheric sulfur injection (in teragram sulfur, TgS)

WAIS-Divide: the ice flow divide on the West Antarctic Ice Sheet (WAIS) which is a linear boundary that separates the region where the ice flows to the Ross Sea, from the region where the ice flows to the Weddell Sea. It is similar to a continental hydrographic divide.

WD: deep ice core drilled at WAIS-Divide

WD2014: WAIS Divide Chronology 2014; chronology developed for the WD ice core, which is based down to 31,000 years before present on annual layer counting on multiple impurity records

**Table S2: Dating assessment using tree-rings. Marker events in which a ring-width minima (Salzer et al., 2014) corresponded with a frost damaged ring within an error margin of  $\pm 1$  year (Salzer and Hughes, 2007) in relation to reconstructed volcanic deposition events over the Late Holocene (this study) and the past 2,500 years (Toohey and Sigl, 2017). WD2014 ages are provided for bipolar eruption signals (Sigl et al., 2016). Ages from attributed Northern Hemisphere extratropical eruptions are on the NS1-2011 chronology (Sigl et al., 2015). All ages are reported using the ISO 8601 international standard, which does (in contrast to the historical Gregorian calendar) include a year 0.**

Ring-width minima year (BCE/CE)	Frost-ring year (BCE/CE)	Cooling start year (BCE/CE)	WD2014 start year (BCE/CE)	eVolv2k start year (BCE/CE)	Age difference (year)	VSSI (Tg S)
-2840	-2840	-2840	no match	N/A	N/A	N/A
-2731	-2730	-2731	no match	N/A	N/A	N/A
-1651	-1652	-1652	<b>-1656</b>	N/A	<b>-4</b>	<b>45</b>
-1625	-1626	-1626	<b>-1628</b>	N/A	<b>-2</b>	<b>23</b>
-1417	-1418	-1418	<b>-1423</b>	N/A	<b>-5</b>	<b>33</b>
-1134	-1134	-1134	-1139	N/A	-5	3
-475	-475	-475	(NHET)	-478	-3	2
-244	-243	-244	-248	-247	-4	9
-41	-42	-42	-47	<b>-44</b>	<b>-5</b>	<b>39</b>
274	273	273	no match	N/A	N/A	N/A
627	627	627	(NHET)	<b>626</b>	<b>-1</b>	<b>13</b>
681	681	681	682	<b>682</b>	<b>1</b>	<b>27</b>
990	989	989	990	990	1	0
1201	1200	1200	(NHET)	1200	0	3
1288	1287	1287	1286	<b>1286</b>	<b>-1</b>	<b>15</b>
1458	1457	1457	1458	<b>1458</b>	<b>1</b>	<b>33</b>
1471	1470	1470	(NHET)	1470	0	1
1578	1577	1577	no match	1576	-1	0
1602	1601	1601	1600	<b>1601</b>	<b>-1</b>	<b>19</b>
1641	1640	1640	1640	<b>1641</b>	<b>0</b>	<b>19</b>
1681	1680	1680	no match	N/A	N/A	N/A

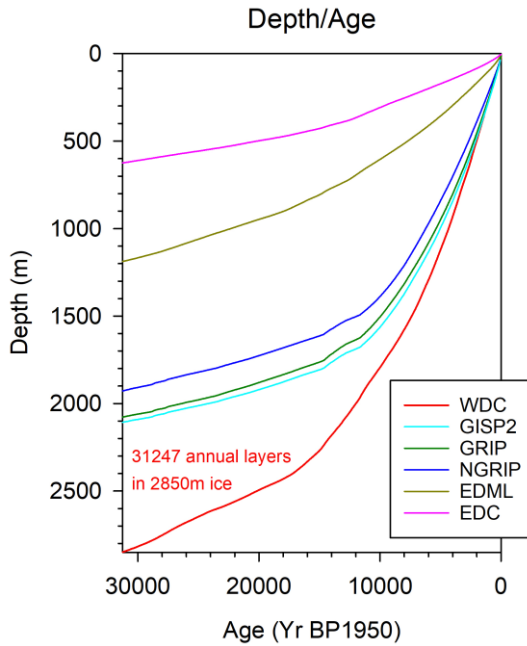


**Figure S1:** Depth-age relationship for six deep ice cores from Antarctica and Greenland discussed in the paper. All ice core records have been transferred to the WD2014 annual-layer counted ice-core chronology (Sigl et al., 2016) using volcanic tie points during the Holocene (this study) and the last Glacial (Svensson et al., 2020).

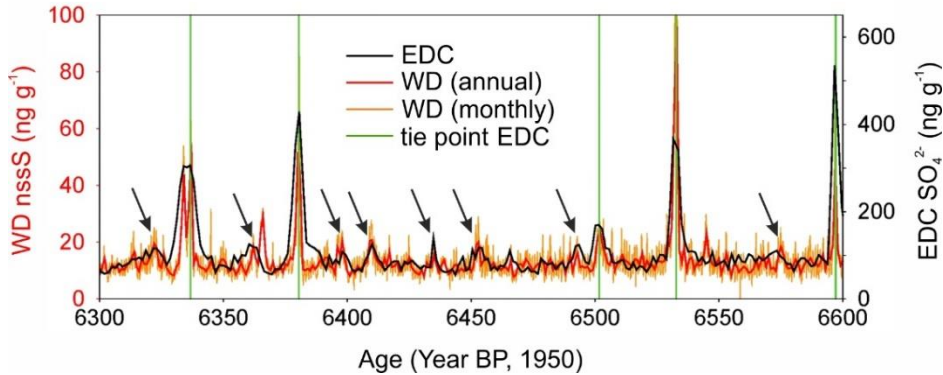


**Figure S2:** Sulfur concentration record from WD (monthly and annual) and EDC ice cores synchronized on the WD chronology using five volcanic tie points (green lines) and linear interpolation. Note that numerous smaller volcanic signals (arrows) are closely aligning without being used as fixed tie points during the first iteration of the synchronization.

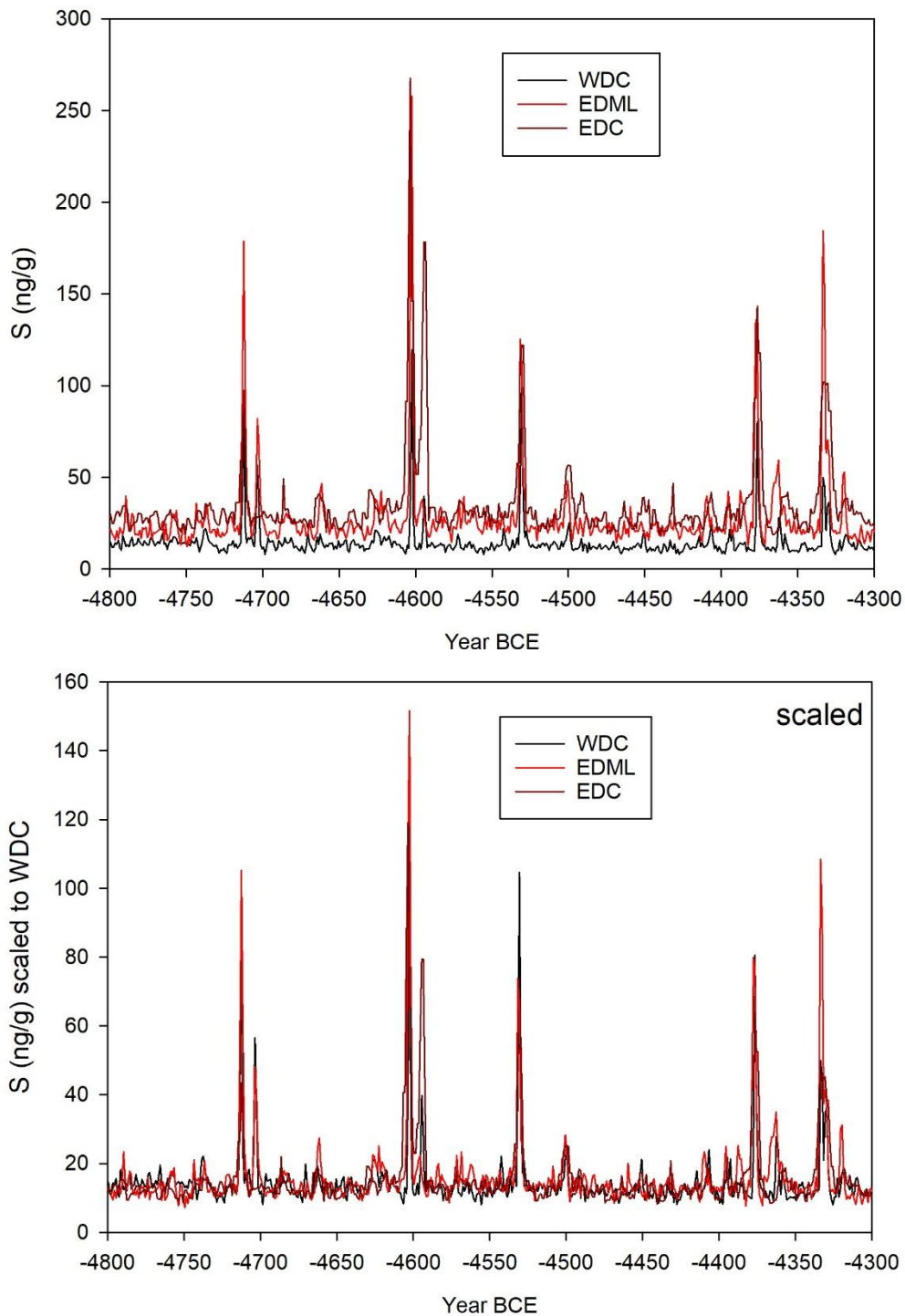


**Figure S3:** (Upper panel): Sulfur concentrations in the three ice cores from Antarctica for a representative time period 4800–4300 BCE. For the EDML and EDC ice cores, sulfur concentrations are derived from sulfate concentration data using  $[S] = [SO_4^{2-}] / 2.996$ . (Lower panel): EDML and EDC were scaled to WDC for better comparability of relative peak magnitudes with respect to the background.

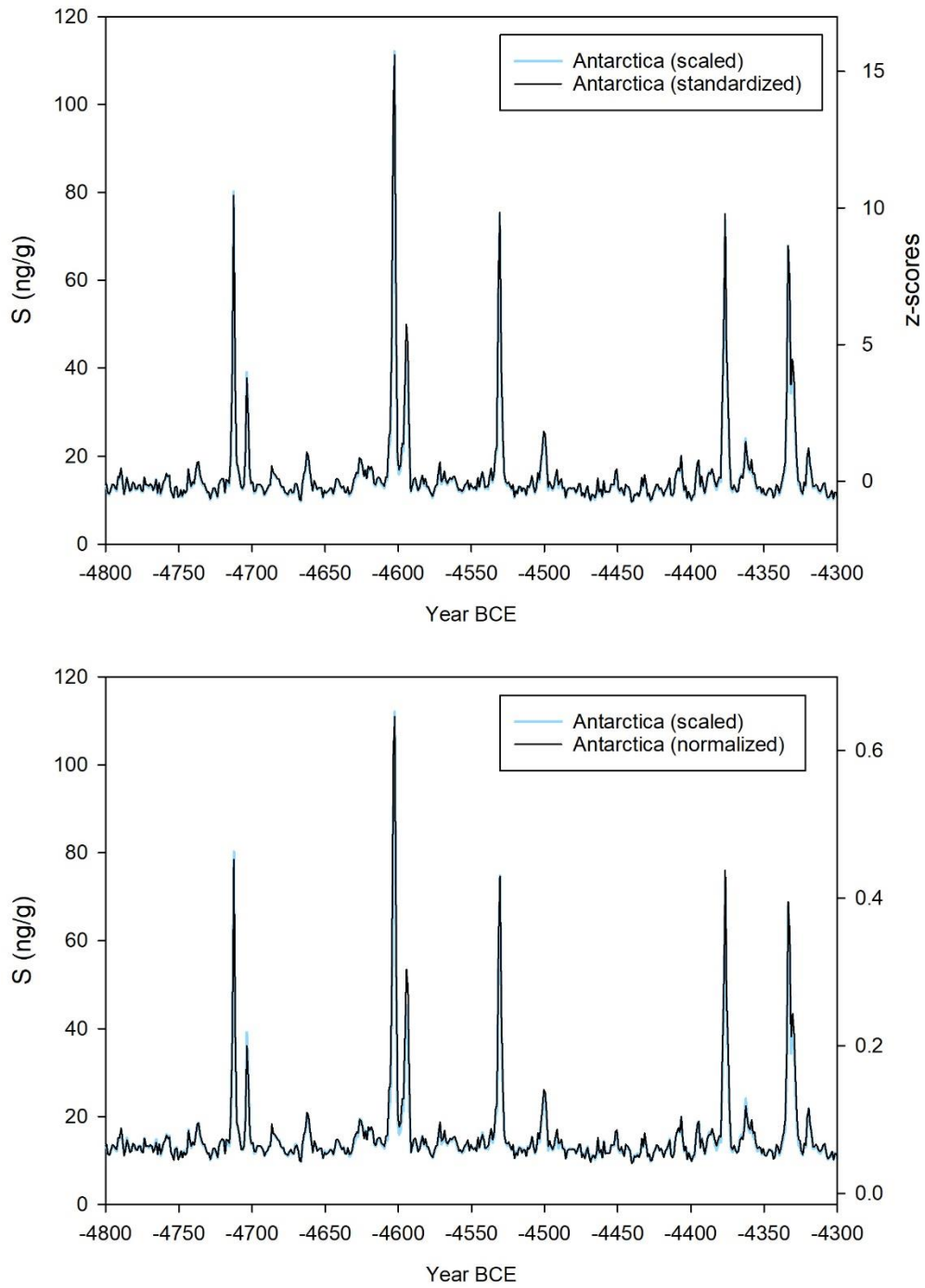


**Figure S4:** (Upper panel): Mean Antarctica (N=3) stacked sulfur concentrations (scaled to WDC, blue) versus stacked standardized Antarctica z-scores (black). (Lower panel) Mean Antarctica (N=3) stacked sulfur concentrations (scaled to WDC, blue) versus normalized concentrations.

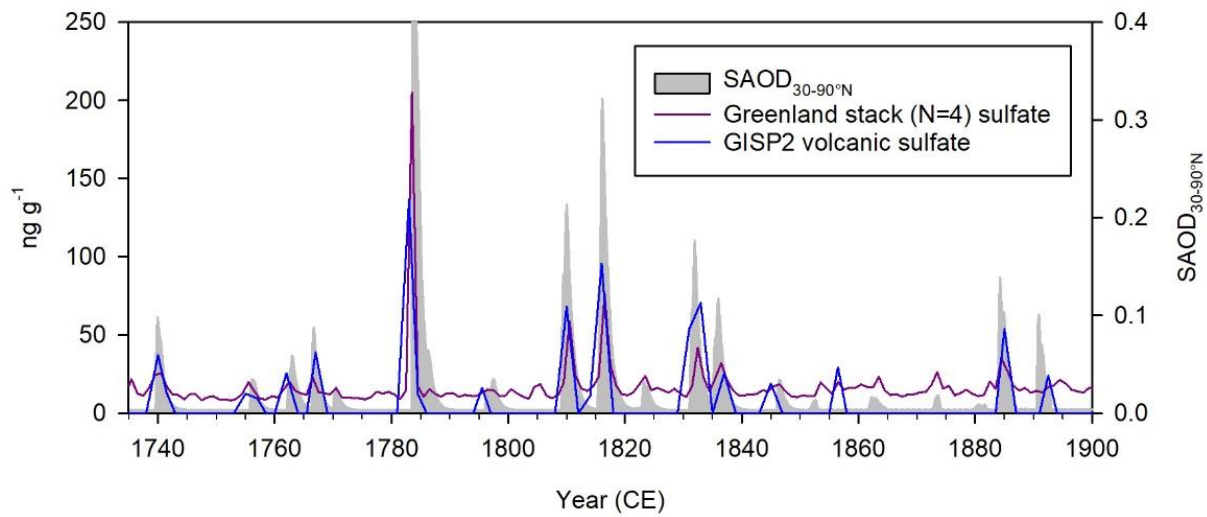


**Figure S5:** Reconstructed stratospheric aerosol optical depth (SAOD) between 30-90°N (Toohey and Sigl, 2017), mean sulfate concentrations from four ice cores (Summit 2010, D4, NEEM-2011-S1, TUNU2013) from Greenland (Maselli et al., 2017; McConnell et al., 2007; Sigl et al., 2013) and volcanic sulfate from GISP2 (Mayewski et al., 1997).

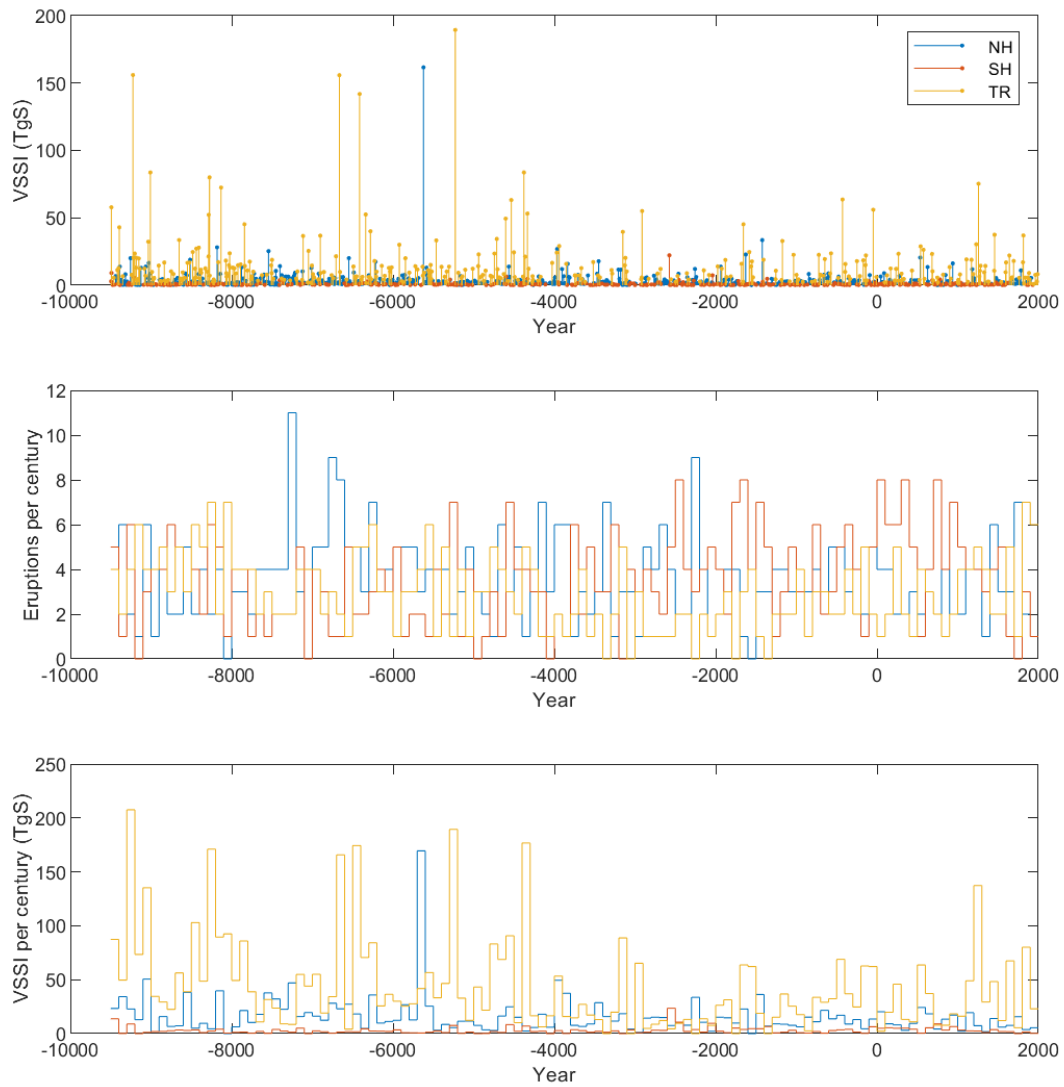


**Figure S6: Holocene volcanic stratospheric sulfur injection (VSSI) from tropical, NH and SH extratropical explosive eruptions. (Top) Reconstructed VSSI for single eruptions over the Holocene, (middle) number of eruptions per century, (bottom) total VSSI per century.**

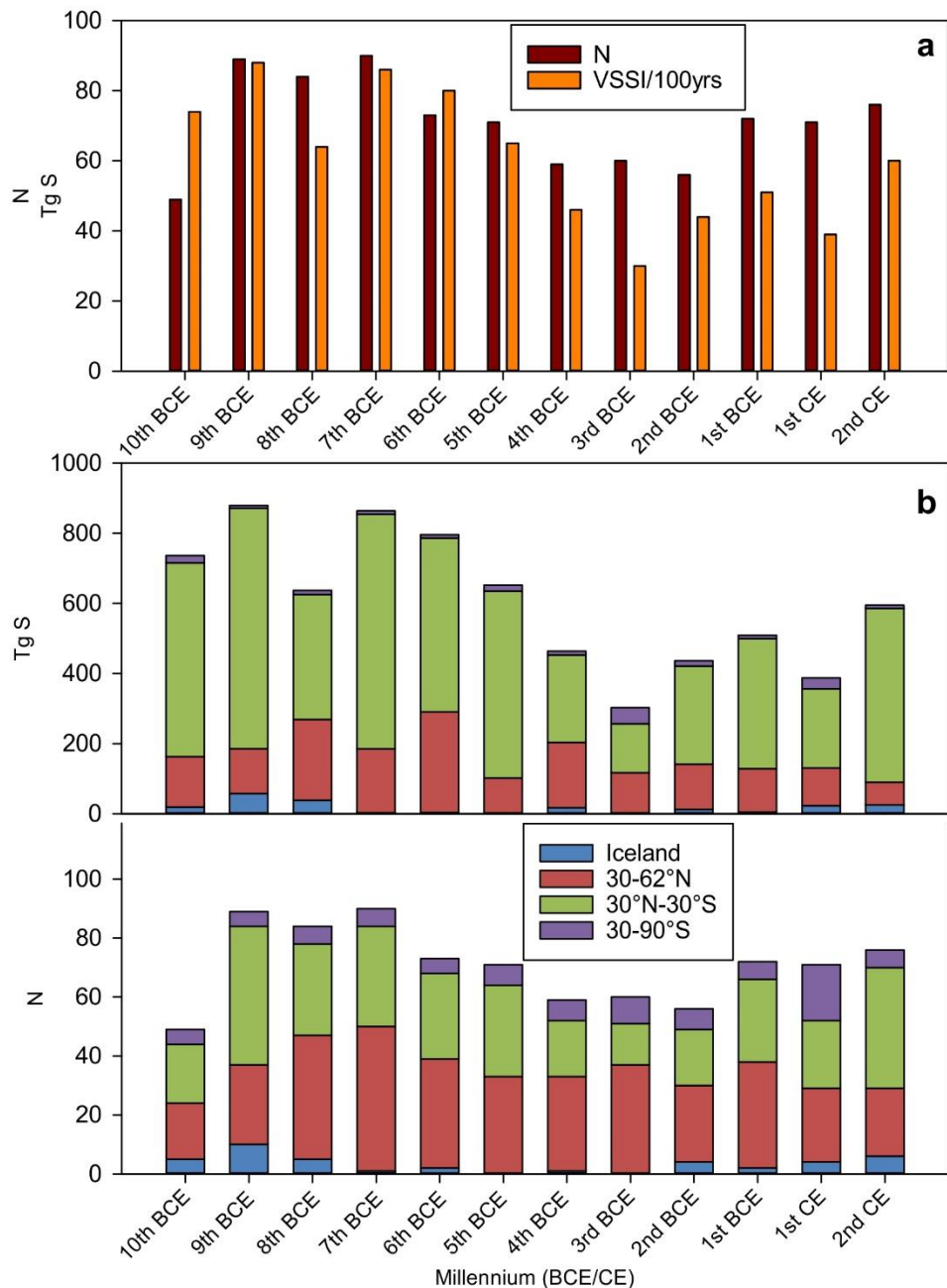


**Figure S7:** a. Total number of volcanic reconstructions and mean volcanic stratospheric sulphur injection (VSSI) per century for each millennia; b. Cumulative VSSI and number of eruptions grouped by their estimated location in Iceland and three latitudinal bands. Only eruptions with VSSI >1 Tg S are included. Note that the value of 10<sup>th</sup> millennia BC only contains eruptions starting in 9500 BCE.

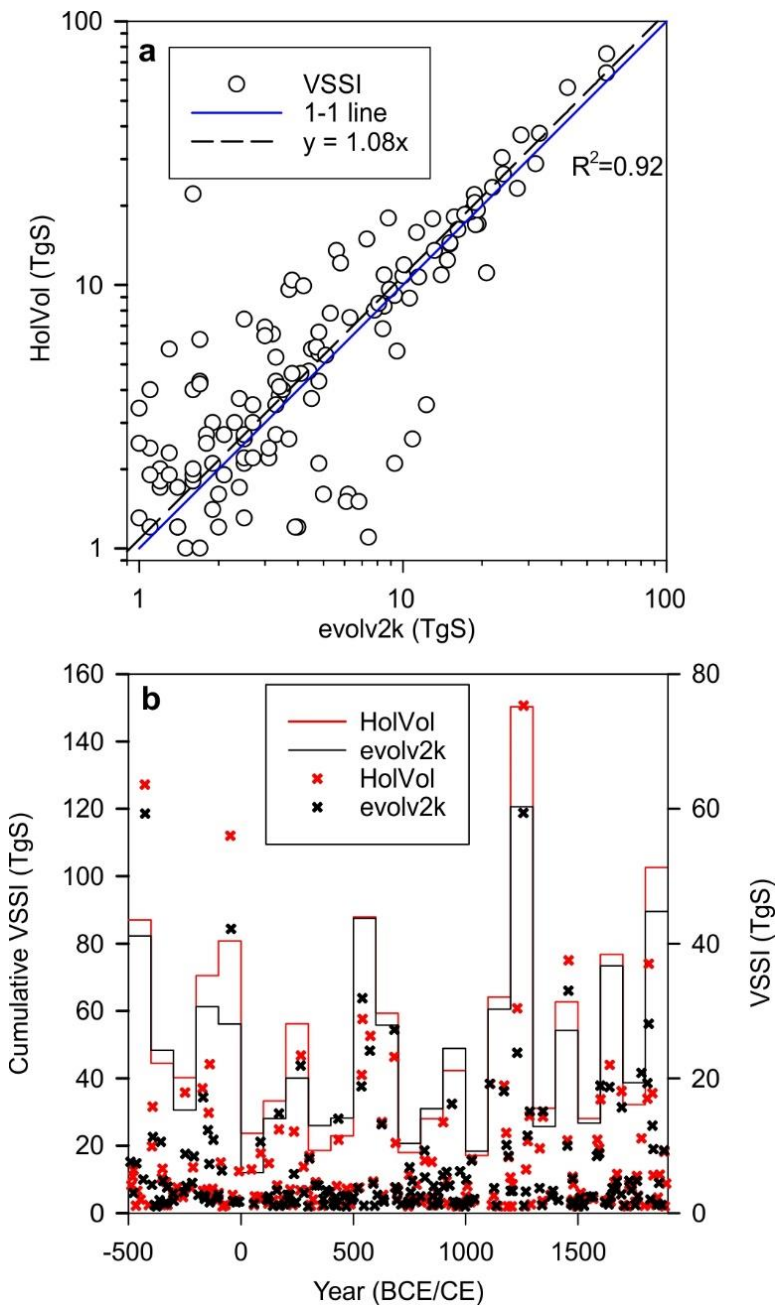


**Figure S8:** a. Scatterplot of volcanic stratospheric sulphur injections (VSSI) during the Common Era in HolVol v.1.0 and evolv2k. b. Cumulative centennial and individual event-integrated (cross) VSSI in HolVol v.1.0 and evolv2k, respectively. Only eruptions with VSSI > 1 Tg S are shown.

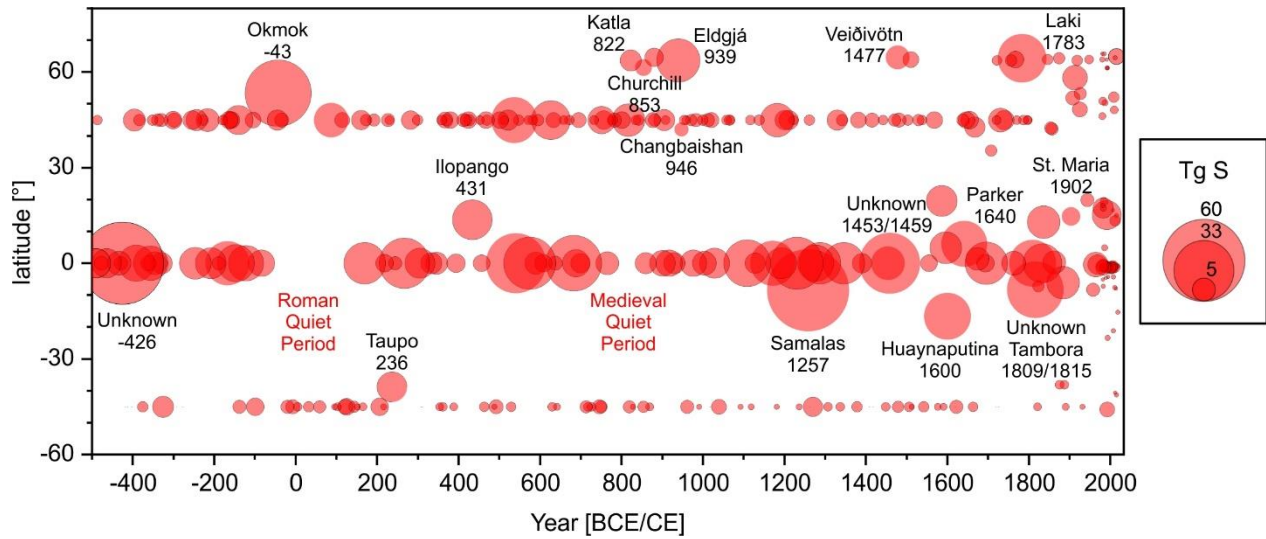


**Figure S9:** Number and volcanic stratospheric sulphur injection (VSSI) of volcanic eruptions over the past 2,500 years from evolv2k (Toohey and Sigl, 2017) grouped by their known and estimated location (NHET 30-90°N; tropics 30°-30°S; SHET 30-90°S). Estimates from 1979 AD onwards are based on satellite retrievals (Carn et al., 2016). Only eruptions with VSSI >1 Tg S are included; source attributions for NHET and for Samalas 1257 CE are based on geochemistry of cryptotephra from Greenland ice cores (Abbott and Davies, 2012; Abbott et al., 2021; Jensen et al., 2014; Lavigne et al., 2013; McConnell et al., 2020; Oppenheimer et al., 2018; Oppenheimer et al., 2017; Plunkett et al., 2020; Smith et al., 2020; Sun et al., 2014).

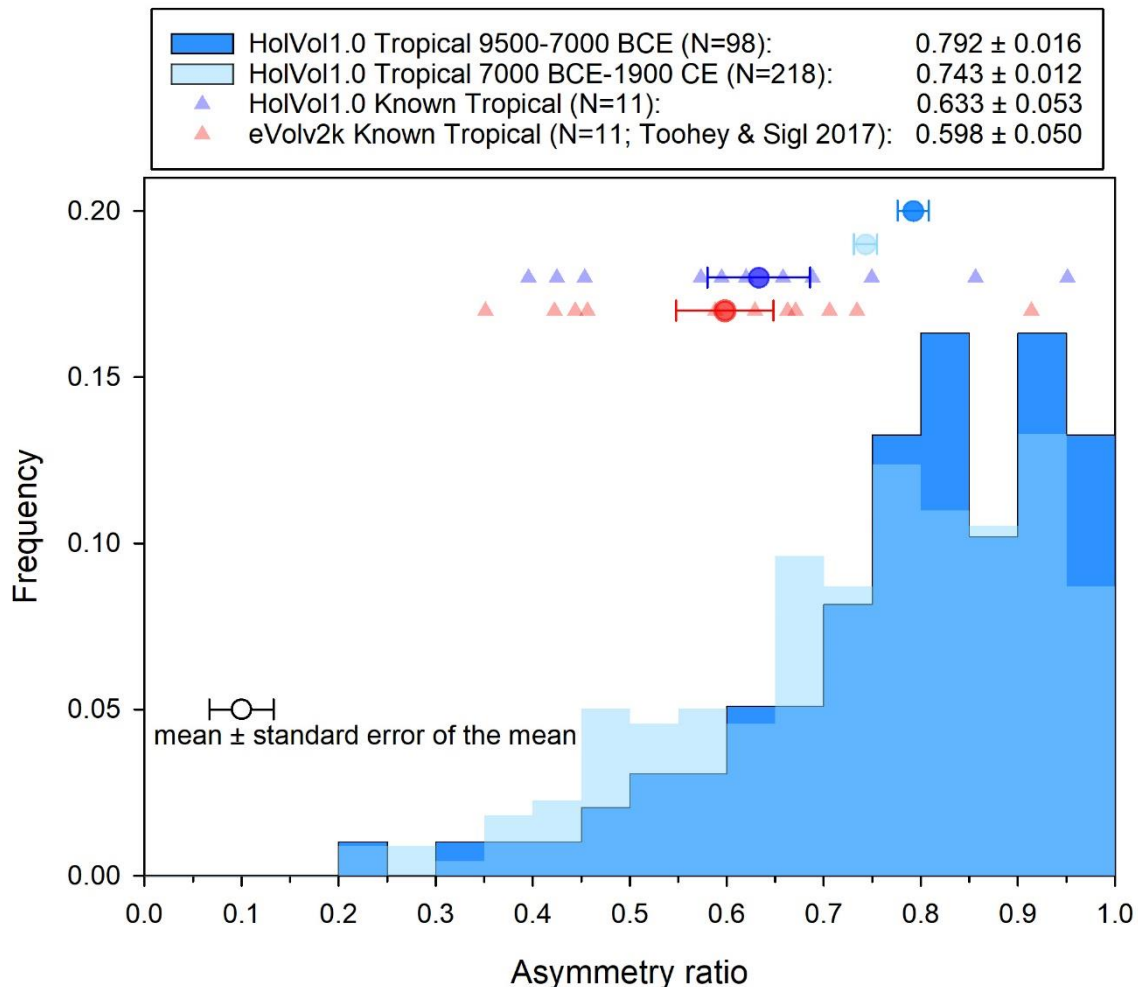


**Figure S10: Distribution of asymmetry ratios [ $DSO4_{GRL}/(DSO4_{GRL} + DSO4_{ANT})$ ] in HolVol1.0 and eVolv2k for attributed tropical eruptions and eleven known tropical eruptions detected in ice cores, where  $DSO4$  is the mean sulfate deposition over Greenland (GRL) and Antarctica (ANT), respectively. High occurrence of asymmetry ratios  $\geq 0.75$  (i.e., with disproportionately strong deposition over Greenland) is observed in particular between 9500-7000 BCE. Also shown are the mean and individual asymmetry ratios for eleven known tropical eruptions attributed to volcanic sulfate signals in HolVol v.1.0 and eVolv2k.**

## Supplementary References

- Abbott, P. M. and Davies, S. M.: Volcanism and the Greenland ice-cores: the tephra record, *Earth-Sci Rev*, 115, 173-191, 2012.
- Abbott, P. M., Plunkett, G., Corona, C., Chellman, N. J., McConnell, J. R., Pilcher, J. R., Stoffel, M., and Sigl, M.: Cryptotephra from the Icelandic Veiðivötn 1477 CE eruption in a Greenland ice core: confirming the dating of volcanic events in the 1450s CE and assessing the eruption's climatic impact, *Clim. Past*, 17, 565-585, 2021.
- Carn, S. A., Clarisse, L., and Prata, A. J.: Multi-decadal satellite measurements of global volcanic degassing, *J Volcanol Geoth Res*, 311, 99-134, 2016.
- Jensen, B. J. L., Pyne-O'Donnell, S., Plunkett, G., Froese, D. G., Hughes, P. D. M., Sigl, M., McConnell, J. R., Amesbury, M. J., Blackwell, P. G., van den Bogaard, C., Buck, C. E., Charman, D. J., Clague, J. J., Hall, V. A., Koch, J., Mackay, H., Mallon, G., McColl, L., and Pilcher, J. R.: Transatlantic distribution of the Alaskan White River Ash, *Geology*, 42, 875-878, 2014.
- Lavigne, F., Degeai, J. P., Komorowski, J. C., Guillet, S., Robert, V., Lahitte, P., Oppenheimer, C., Stoffel, M., Vidal, C. M., Surono, Pratomo, I., Wassmer, P., Hajdas, I., Hadmoko, D. S., and De Belizal, E.: Source of the great A.D. 1257 mystery eruption unveiled, Samalas volcano, Rinjani Volcanic Complex, Indonesia, *P Natl Acad Sci USA*, 110, 16742-16747, 2013.
- Maselli, O. J., Chellman, N. J., Grieman, M., Layman, L., McConnell, J. R., Pasteris, D., Rhodes, R. H., Saltzman, E. S., and Sigl, M.: Sea ice and pollution-modulated changes in Greenland ice core methanesulfonate and bromine, *Clim Past*, 13, 39-59, 2017.
- Mayewski, P. A., Meeker, L. D., Twickler, M. S., Whitlow, S., Yang, Q. Z., Lyons, W. B., and Prentice, M.: Major features and forcing of high-latitude northern hemisphere atmospheric circulation using a 110,000-year-long glaciochemical series, *J Geophys Res-Oceans*, 102, 26345-26366, 1997.
- McConnell, J. R., Edwards, R., Kok, G. L., Flanner, M. G., Zender, C. S., Saltzman, E. S., Banta, J. R., Pasteris, D. R., Carter, M. M., and Kahl, J. D. W.: 20th-century industrial black carbon emissions altered arctic climate forcing, *Science*, 317, 1381-1384, 2007.
- McConnell, J. R., Sigl, M., Plunkett, G., Burke, A., Kim, W., Raible, C. C., Wilson, A. I., Manning, J. G., Ludlow, F. M., Chellman, N. J., Innes, H. M., Yang, Z., Larsen, J. F., Schaefer, J. R., Kipfstuhl, S., Mojtabavi, S., Wilhelms, F., Opel, T., Meyer, H., and Steffensen, J. P.: Extreme climate after massive eruption of Alaska's Okmok volcano in 43 BCE and effects on the late Roman Republic and Ptolemaic Kingdom, *Proceedings of the National Academy of Sciences*, 2020.
- Oppenheimer, C., Orchard, A., Stoffel, M., Newfield, T. P., Guillet, S., Corona, C., Sigl, M., Di Cosmo, N., and Buntgen, U.: The Eldgja eruption: timing, long-range impacts and influence on the Christianisation of Iceland, *Climatic Change*, 147, 369-381, 2018.

- Oppenheimer, C., Wacker, L., Xu, J., Galvan, J. D., Stoffel, M., Guillet, S., Corona, C., Sigl, M., Di Cosmo, N., Hajdas, I., Pan, B., Breuker, R., Schneider, L., Esper, J., Fei, J., Hammond, J. O. S., and Büntgen, U.: Multi-proxy dating the ‘Millennium Eruption’ of Changbaishan to late 946 CE, *Quaternary Sci Rev*, 158, 164-171, 2017.
- Plunkett, G., Sigl, M., Pilcher, J. R., McConnell, J. R., Chellman, N., Steffensen, J. P., and Büntgen, U.: Smoking guns and volcanic ash: the importance of sparse tephras in Greenland ice cores, *Polar Res*, 2020, 2020.
- Salzer, M. W., Bunn, A. G., Graham, N. E., and Hughes, M. K.: Five millennia of paleotemperature from tree-rings in the Great Basin, USA, *Clim Dynam*, 42, 1517-1526, 2014.
- Salzer, M. W. and Hughes, M. K.: Bristlecone pine tree rings and volcanic eruptions over the last 5000 yr, *Quaternary Res*, 67, 57-68, 2007.
- Sigl, M., Fudge, T. J., Winstrup, M., Cole-Dai, J., Ferris, D., McConnell, J. R., Taylor, K. C., Welten, K. C., Woodruff, T. E., Adolphi, F., Bisiaux, M., Brook, E. J., Buizert, C., Caffee, M. W., Dunbar, N. W., Edwards, R., Geng, L., Iverson, N., Koffman, B., Layman, L., Maselli, O. J., McGwire, K., Muscheler, R., Nishiizumi, K., Pasteris, D. R., Rhodes, R. H., and Sowers, T. A.: The WAIS Divide deep ice core WD2014 chronology - Part 2: Annual-layer counting (0-31 ka BP), *Clim Past*, 12, 769-786, 2016.
- Sigl, M., McConnell, J. R., Layman, L., Maselli, O., McGwire, K., Pasteris, D., Dahl-Jensen, D., Steffensen, J. P., Vinther, B., Edwards, R., Mulvaney, R., and Kipfstuhl, S.: A new bipolar ice core record of volcanism from WAIS Divide and NEEM and implications for climate forcing of the last 2000 years, *J Geophys Res-Atmos*, 118, 1151-1169, 2013.
- Sigl, M., Winstrup, M., McConnell, J. R., Welten, K. C., Plunkett, G., Ludlow, F., Büntgen, U., Caffee, M., Chellman, N., Dahl-Jensen, D., Fischer, H., Kipfstuhl, S., Kostick, C., Maselli, O. J., Mekhaldi, F., Mulvaney, R., Muscheler, R., Pasteris, D. R., Pilcher, J. R., Salzer, M., Schupbach, S., Steffensen, J. P., Vinther, B. M., and Woodruff, T. E.: Timing and climate forcing of volcanic eruptions for the past 2,500 years, *Nature*, 523, 543-549, 2015.
- Smith, V. C., Costa, A., Aguirre-Díaz, G., Pedrazzi, D., Scifo, A., Plunkett, G., Poret, M., Tournigand, P.-Y., Miles, D., Dee, M. W., McConnell, J. R., Sunyé-Puchol, I., Harris, P. D., Sigl, M., Pilcher, J. R., Chellman, N., and Gutiérrez, E.: The magnitude and impact of the 431 CE Tierra Blanca Joven eruption of Ilopango, El Salvador, *Proceedings of the National Academy of Sciences*, doi: 10.1073/pnas.2003008117, 202003008, 2020.
- Sun, C. Q., Plunkett, G., Liu, J. Q., Zhao, H. L., Sigl, M., McConnell, J. R., Pilcher, J. R., Vinther, B., Steffensen, J. P., and Hall, V.: Ash from Changbaishan Millennium eruption recorded in Greenland ice: Implications for determining the eruption's timing and impact, *Geophys Res Lett*, 41, 694-701, 2014.
- Svensson, A., Dahl-Jensen, D., Steffensen, J. P., Blunier, T., Rasmussen, S. O., Vinther, B. M., Vallelonga, P., Capron, E., Gkinis, V., Cook, E., Kjaer, H. A., Muscheler, R., Kipfstuhl, S., Wilhelms, F., Stocker, T. F., Fischer, H., Adolphi, F., Erhardt, T., Sigl, M., Landais, A., Parrenin, F., Buizert, C., McConnell, J. R., Severi, M., Mulvaney, R., and Bigler, M.: Bipolar volcanic synchronization of abrupt climate change in Greenland and Antarctic ice cores during the last glacial period, *Clim Past*, 16, 1565-1580, 2020.

Toohey, M. and Sigl, M.: Volcanic stratospheric sulfur injections and aerosol optical depth from 500 BCE to 1900 CE,  
*Earth System Science Data*, 9, 809-831, 2017.